Osmosensitive Changes of Carbohydrate Metabolism in Response to Cellulose Biosynthesis Inhibition[1][W][OA]

Alexandra Wormit[2], Salman M. Butt, Issariya Chairam, Joseph F. McKenna, Adriano Nunes-Nesi[3], Lars Kjaer, Kerry O'Donnelly, Alisdair R. Fernie, Rüdiger Woscholski, M.C. Laura Barter, and Thorsten Hamann*

Division of Cell and Molecular Biosciences, Faculty of Natural Sciences (A.W., I.C., J.F.M., L.K., T.H.), and Chemical Biology Section, Department of Chemistry and Institute of Chemical Biology (S.M.B., K.O., R.W., M.C.L.B.), Imperial College London, South Kensington Campus, London SW7 2AZ, United Kingdom; Rheinisch-Westfälische Technische Hochschule Aachen, Institut Biologie I, Worringer Weg 1, D–52056 Aachen, Germany (A.W.); and Max Planck Institute of Molecular Plant Physiology, 14476 Potsdam-Golm, Germany (A.N.-N., A.R.F.)

Cellulose is the most abundant biopolymer in the world, the main load-bearing element in plant cell walls, and represents a major sink for carbon fixed during photosynthesis. Previous work has shown that photosynthetic activity is partially regulated by carbohydrate sinks. However, the coordination of cellulose biosynthesis with carbohydrate metabolism and photosynthesis is not well understood. Here, we demonstrate that cellulose biosynthesis inhibition (CBI) leads to reductions in transcript levels of genes involved in photosynthesis, the Calvin cycle, and starch degradation in Arabidopsis (*Arabidopsis thaliana*) seedlings. In parallel, we show that CBI induces changes in carbohydrate distribution and influences Rubisco activase levels. We find that the effects of CBI on gene expression and carbohydrate metabolism can be neutralized by osmotic support in a concentration-dependent manner. However, osmotic support does not suppress CBI-induced metabolic changes in seedlings impaired in mechanoperception (*mid1 complementing activity1* [*mca1*]) and osmoperception (*cytokinin receptor1* [*cre1*]) or reactive oxygen species production (*respiratory burst oxidase homolog DF* [*rbohDF*]). These results show that carbohydrate metabolism is responsive to changes in cellulose biosynthesis activity and turgor pressure. The data suggest that MCA1, CRE1, and RBOHDF-derived reactive oxygen species are involved in the regulation of osmosensitive metabolic changes. The evidence presented here supports the notion that cellulose and carbohydrate metabolism may be coordinated via an osmosensitive mechanism.

Plant cell walls form the bulk of the lignocellulosic biomass that has been identified as a source for the sustainable production of energy. Lignin and cellulose biosynthesis produce the main load-bearing elements of primary and secondary plant cell walls and represent major sinks for photosynthesis products (Paul and Foyer, 2001; Hancock et al., 2007; Demura and Ye, 2010). There have been a number of observations that support the long-held view that photosynthetic activity, primary metabolism, and carbon sinks, such as lignin biosynthesis, are coordinated and that photosynthesis is partially sink regulated. Examples include the RNA interference-based suppression of *p*-coumaroyl-CoA 3′-hydroxylase, which leads to a reduction of photosynthetic carbon assimilation and increased levels of photosynthate in leaves (Rogers et al., 2005; Coleman et al., 2008), and the observation that the *starch excess1* mutant exhibits reduced lignin accumulation while being impaired in starch turnover (Rogers et al., 2005). Very little is known about the mechanisms coordinating cellulose production with primary metabolism and photosynthesis.

Different mechanisms and regulators, which have been shown to control carbohydrate metabolism, are reviewed by Stitt et al. (2010) and Geigenberger (2011). Examples include (1) allosteric regulation of enzymes by metabolic intermediates, as demonstrated for AGPase or cytosolic Fru-1,6-bisphosphatase (Ghosh and Preiss, 1966); (2) regulation by posttranslational redox modulation shown by several enzymes involved in starch metabolism, such as α-GLUCAN WATER DIKINASE1

[1] This work was supported by a Marie Curie Postdoctoral Fellowship (to A.W.), the Biotechnology and Biological Sciences Research Council (doctoral training fellowship to J.F.M.), Ph.D. fellowships from the Royal Thai Government (to I.C.), the Porter Institute at Imperial College London (to L.K.), and the Engineering and Physical Sciences Research Council, funded by the Centre for Doctoral Training of the Institute of Chemical Biology, Imperial College London (to K.O.), the Max Planck Gesellschaft (A.R.F. and A.N.-N.), and the Royal Society (L.M.C.B.).

[2] Present address: Rheinisch-Westfälische Technische Hochschule Aachen, Institut Biologie I, Worringerweg 1, D–52056 Aachen, Germany.

[3] Present address: Departmento de Biologia Vegetal, Universidade Federal de Viçosa, 36570-000 Viçosa, Brazil.

* Corresponding author; e-mail thamann@imperial.ac.uk.

The author responsible for distribution of materials integral to the findings presented in this article in accordance with the policy described in the Instructions for Authors (www.plantphysiol.org) is: T. Hamann (thamann@imperial.ac.uk).

[W] The online version of this article contains Web-only data.

[OA] Open Access articles can be viewed online without a subscription.

www.plantphysiol.org/cgi/doi/10.1104/pp.112.195198

(GWD1), an enzyme required for starch degradation (Geigenberger et al., 2005; Mikkelsen et al., 2005); and (3) regulatory changes in the expression of genes involved in starch metabolism in sink and source tissues, reported in different plant species such as barley (*Hordeum vulgare*), Arabidopsis (*Arabidopsis thaliana*), and potato (*Solanum tuberosum*), which appear to be influenced by soluble sugar levels (Smith et al., 2004; Bläsing et al., 2005; Osuna et al., 2007; Kloosterman et al., 2008; Mangelsen et al., 2010).

Several examples for the adaptation of metabolic processes in plants to environmental change have been discussed recently (Geigenberger, 2011). Arabidopsis plants respond to drought and hyperosmotic stress with abscisic acid (ABA)-dependent changes in carbohydrate distribution (Kempa et al., 2008). In water-stressed potato tubers, starch synthesis and cell wall formation are reduced whereas Suc levels are increased (Oparka and Wright, 1988a, 1988b). Suc phosphate synthase and AGPase have been identified as key enzymes required to bring about these metabolic changes (Geigenberger et al., 1999a). However, the mechanisms translating environmental perturbation into a response in terms of enzyme activity and/or adaptation of carbohydrate metabolism are not well understood (Gupta and Kaur, 2005; Kempa et al., 2007; Hey et al., 2010).

Recent publications have shown that plants have evolved a mechanism to monitor the functional integrity of the cell wall and initiate changes in wall composition/structure and cellular metabolism to maintain wall integrity in response to environmental perturbations (Seifert and Blaukopf, 2010). A similar cell wall integrity mechanism exists in *Saccharomyces cerevisiae*, and it has been shown that the functional integrity of the yeast cell wall is maintained by three different signaling mechanisms (Levin, 2005). The first consists of plasma membrane-localized proteins, such as WSC1, which have extracellular domains capable of sensing physical cell wall damage and creating a signal that is relayed through the G-protein RHO1, PKC1 protein kinase, and a mitogen-activated protein kinase cascade. The second signaling system consists of the yeast osmosensing system based on SLN1 and SHO1, which uses YPD1 to regulate the expression of response genes (Lu et al., 2003). The third consists of a stretch-activated, plasma membrane-localized calcium channel complex formed by CCH1 and MID1, which generates a signal relayed via calcineurin and CRZ1 (Fischer et al., 1997). Interestingly, the MID1 COMPLEMENTING ACTIVITY1 (MCA1) protein from Arabidopsis can partially rescue a *MID1*-deficient yeast strain, while another Arabidopsis protein, CYTOKININ RECEPTOR1 (CRE1), can complement an SLN1-deficient strain in the presence of cytokinin (Inoue et al., 2001; Reiser et al., 2003; Levin, 2005; Nakagawa et al., 2007). Recently, it has been shown that MCA1 and RESPIRATORY BURST OXIDASE HOMOLOG DF (RBOHDF)-derived reactive oxygen species (ROS) are required to initiate lignin production induced by cellulose biosynthesis inhibition (CBI) in Arabidopsis seedling roots and that the lignin deposition can be suppressed by osmotic support (Hamann et al., 2009; Denness et al., 2011). These results suggest that similarities exist at the functional and organizational levels between the plant and yeast cell wall integrity maintenance mechanisms.

The aim of the work presented here was to analyze the short-term impact of CBI on carbohydrate metabolism/photosynthetic activity and to characterize the mechanism regulating these processes. To achieve this goal, we have used two cellulose biosynthesis inhibitors, isoxaben (ISX) and dichlobenil (DCB), with different modes of action. The highly specific preemergence herbicide ISX causes CBI during primary cell wall formation (Scheible et al., 2001; Hématy et al., 2007; Hamann et al., 2009; Tsang et al., 2011). All the mutations causing resistance or hypersensitivity to ISX affect components of the cellulose synthase complex active during primary cell wall formation, highlighting the specificity of the inhibitor. Another efficient and well-established cellulose biosynthesis inhibitor that was used here is DCB. This inhibitor reduces the activity of cellulose synthase complexes possibly by affecting the interaction of the complexes with the cytoskeleton (Delmer, 1999; Himmelspach et al., 2003; Rajangam et al., 2008). Our results show that CBI causes a transient redistribution of carbohydrate, reveal a regulatory role for turgor pressure, and implicate several genes in mediating the osmosensitive process.

RESULTS

CBI Affects the Expression of Genes Involved in Photosynthesis and Starch Metabolism

DNA microarray-based expression profiling of Arabidopsis seedlings exposed to CBI suggested global changes in transcript levels after 4 h (Hamann et al., 2009). The expression of several genes involved in photosynthesis and starch metabolism appeared down-regulated in response to inhibitor treatment (Supplemental Fig. S1). Examples include genes encoding components of the LIGHT-HARVESTING ANTENNA COMPLEX (LHC) of PSI and PSII, *RUBISCO ACTIVASE*, *CHAPERONIN 60β* (*CPN60B*), *PLASTID TRANSCRIPTIONALLY ACTIVE14*, and *GLYCERALDEHYDE-3-PHOSPHATE DEHYDROGENASE B SUBUNIT* (*GAPB*), which are involved in photosynthetic carbon fixation. Other genes apparently affected are involved in starch metabolism, such as *PHOSPHOGLUCOMUTASE*, *STARCH SYNTHASE3*, *ADP-GLC PYROPHOSPHORYLASE LARGE SUBUNIT1*, *GWD1*, *α -GLUCAN PHOSPHORYLASE1*, *DISPROPORTIONATING ENZYME1* (*DPE1*), *STARCH-BRANCHING ENZYME2.2*, and *ISOAMYLASE2* (*ISA2*). To confirm the microarray-derived expression data, time-course experiments using similar experimental conditions were set up and quantitative reverse transcription

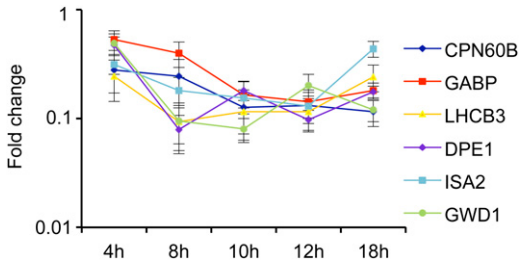

Figure 1. qRT-PCR-based expression analysis of genes involved in carbohydrate metabolism in ISX-treated seedlings. The *x* axis represents time in hours, while the *y* axis shows expression level changes (ISX-treated versus mock-treated control seedlings). Values are means ± SE from three biological replicates.

(qRT)-PCR-based expression profiling of six representative genes involved in carbohydrate metabolism and photosynthesis was performed. This time-course expression analysis confirmed the previous data by showing that the expression of *CPN60B*, *GAPB*, *LHCB3*, *DPE1*, *ISA2*, and *GWD1* was down-regulated after 4 h of ISX treatment (Fig. 1). To confirm that the results obtained were not caused by an unspecific side effect of the inhibitor, the same experimental setup was used but DCB was employed to inhibit cellulose biosynthesis (Supplemental Fig. S2). DCB treatment also resulted in reductions of transcript levels, but the changes were delayed and not as pronounced as with ISX. To summarize, the expression analysis shows that two different cellulose biosynthesis inhibitors cause reductions in the expression of genes involved in starch metabolism and photosynthesis.

CBI Apparently Inhibits the Activity of Rubisco and Affects the Distribution of Carbohydrates

The gene expression profiling experiments (Fig. 1; Supplemental Figs. S1 and S2) revealed that CBI treatment reduced the expression of genes associated with Rubisco activity and the Calvin cycle, thus suggesting that the inhibitor treatment might affect photosynthetic activity. To test this hypothesis, an ELISA-based assay was developed to quantify the levels of Rubisco activase in seedlings mock or inhibitor treated. It was found that the ISX but not the DCB treatment caused a significant reduction in activase levels (Fig. 2A, black bar; Supplemental Table S3).

To determine whether CBI-induced changes in transcript levels affect primary metabolism, metabolic profiling using ^{14}C-labeled Suc was carried out at two time points (Fig. 2B; Supplemental Fig. S3) that were selected based on the expression changes observed (Fig. 1). ISX was used in these experiments, since it has a more direct effect on gene expression. After 8 h, no significant differences between mock- and ISX-treated seedlings were detected for hexose phosphates, flux to glycolysis, and metabolized Suc levels (Supplemental Fig. S3). However, Suc uptake and flux to protein were reduced in CBI-treated seedlings. Metabolic flux to starch was slightly increased, whereas flux to the wall was slightly decreased (Supplemental Fig. S3). This led to a significant reduction in the ratio of flux to cell wall versus flux to starch in CBI-treated seedlings after 8 h (Fig. 2B). After 12 h, no significant differences were observed in hexose phosphates and metabolized Suc (Fig. 2B; Supplemental Fig. S3). Suc uptake, flux to glycolysis, and flux to protein were reduced in CBI-treated seedlings compared with mock-treated controls. Flux to starch and flux to cell wall did not differ significantly between mock- and CBI-treated seedlings (Supplemental Fig. S3).

The flux measurements suggested a rerouting of metabolism and possibly a redistribution of soluble sugars and starch in CBI-treated seedlings. To follow up on these observations, time-course experiments were performed and soluble sugars as well as starch contents were quantified in mock-, ISX-, and DCB-treated seedlings (Fig. 2, C–F; Supplemental Fig. S4). Suc concentrations increased in both mock- and ISX-treated seedlings initially but declined more rapidly in ISX-treated seedlings (Fig. 2C). This initial increase may be due to the provision of fresh medium containing Suc at the beginning of the treatment. Glc and Fru accumulated transiently in mock-treated seedlings during the first 10 h of treatment, whereas the ISX-treated seedlings did not exhibit such changes during the same period (Fig. 2, D and E). By contrast to the changes in soluble sugars, ISX-treated seedlings accumulated transiently more starch compared with mock-treated ones, particularly after 8 and 10 h of treatment (Fig. 2F). Analysis of the data deriving from DCB-treated seedlings showed similar but delayed effects regarding changes both in transcript levels and carbohydrate distribution. Suc levels increased in mock- and DCB-treated seedlings initially similarly and then started to diverge after 10 h, with mock-treated seedlings having higher levels than DCB-treated ones (Supplemental Fig. S4A). After 8 h, Glc and Fru levels started to differ between mock- and DCB-treated seedlings (Supplemental Fig. S4, B and C). In contrast, increases in starch levels were more pronounced in DCB- than in mock-treated seedlings after 8 to 10 h (Supplemental Fig. S4D). These observations are similar to the effects observed in DCB-treated seedlings. Changes in the expression of the genes analyzed are delayed compared with ISX-treated seedlings (compare Fig. 1 and Supplemental Fig. S2).

The results presented above suggest that CBI affects Rubisco activase levels and carbohydrate distribution. However, it is important to rule out any response that may be due to unspecific effects of the inhibitors used. Several mutants have been described that exhibit enhanced resistance to ISX (Scheible et al., 2001; Desprez et al., 2002). The mutation in *isoxaben resistant1* (*ixr1-1*) causes an amino acid exchange in the cytoplasmic domain of *CELLULOSE SYNTHASE3*, increasing resistance to ISX by approximately 300-fold. Therefore, *ixr1* was selected to confirm that the observed

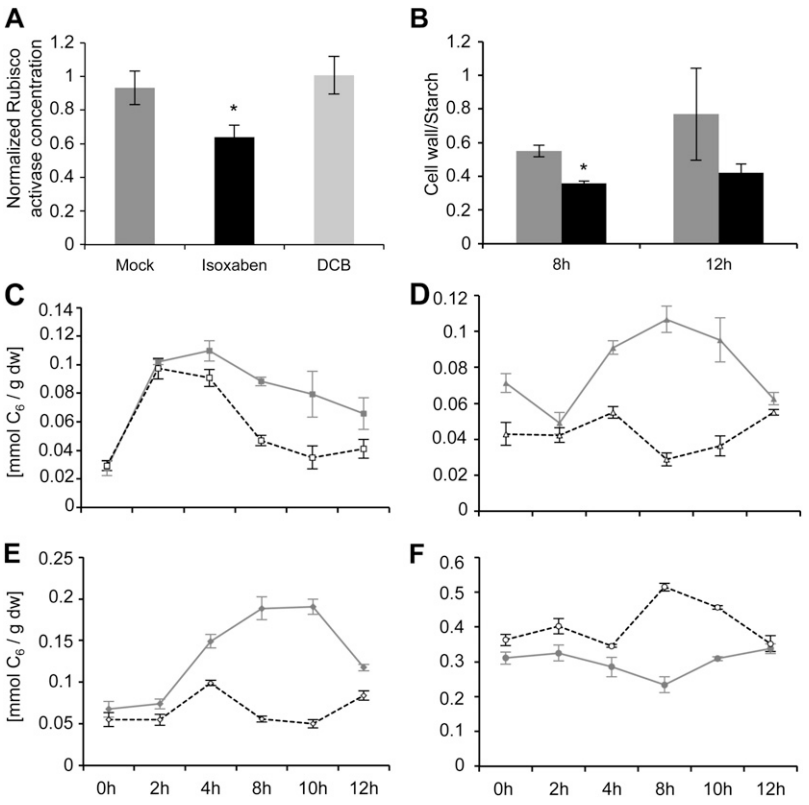

Figure 2. Rubisco activase levels, metabolic flux, soluble sugar, and starch levels in mock- or CBI-treated Col-0 seedlings. A, Seedlings were mock treated (dark gray bar), ISX treated (black bar), or DCB treated (light gray bar) for 10 h. The *y* axis shows the normalized Rubisco activase level for each treatment calculated by determining the ratio of the Rubisco activase concentration after 10 h of treatment to the corresponding 0-h concentration. Error bars are based on six biological replicates and three technical replicates. B, Metabolic flux measurements using ^{14}C-labeled Suc. Each column represents the ratio of flux into cell wall versus flux into starch in seedlings after 8 and 12 h of mock (gray bars) and ISX (black bars) treatment. C to F, Levels of soluble sugars and starch in mock-treated (solid gray lines) and ISX-treated (dashed black lines) seedlings. C, Suc. D, Fru. E, Glc. F, Starch. The *y* axis shows levels of soluble sugars or starch in mmol C_6 g^{-1} dry weight (dw). Error bars represent SD. Asterisks indicate statistically significant differences compared with mock-treated Col-0 samples.

phenotypic effects are caused specifically by ISX (Scheible et al., 2001). Rubisco activase levels were measured in ecotype Columbia (Col-0) and *ixr1-1* seedlings mock or ISX treated for 10 h. The measurements showed that ISX treatment reduces Rubisco activase levels in Col-0. Rubisco activase levels were reduced in mock-treated *ixr1-1* seedlings compared with the Col-0 control (Fig. 3A). More importantly, Rubisco activase levels were not reduced in *ixr1-1* seedlings after ISX treatment. In parallel, soluble sugar and starch levels were determined in Col-0 and *ixr1-1* seedlings mock or ISX treated for 10 h (Fig. 3B; Supplemental Table S1). The ISX treatment reduced the levels of soluble sugars in Col-0 seedlings compared with mock-treated ones, while the starch levels were increased (Fig. 3B, hatched bars; expressed as the ratio of ISX- to mock-treated seedlings). The ISX treatment did not induce changes in soluble sugar and starch levels in *ixr1-1* seedlings compared with the corresponding mock-treated controls (Fig. 3B, black bars). Interestingly, the absolute amounts of both soluble sugars and starch were reduced in the mock-treated

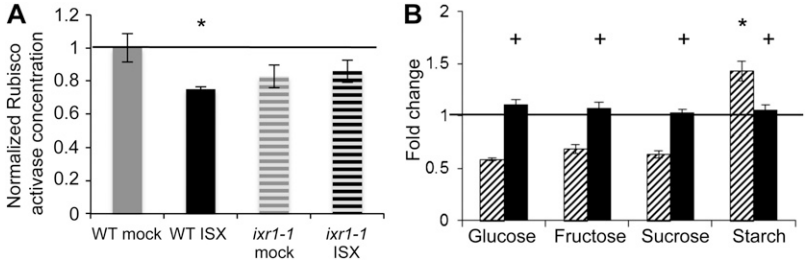

Figure 3. Measurements of Rubisco activase levels and soluble sugar/starch levels in Col-0 and *ixr1-1* seedlings. A, Seedlings were mock treated (gray bars) or ISX treated (black bars). Normalized Rubisco activase levels for each treatment were calculated by determining the ratio of the Rubisco activase concentration after 10 h of treatment to the corresponding 0-h concentration. Error bars are based on six biological replicates and three technical replicates. B, Data from ISX-treated Col-0 (hatched bars) and *ixr1-1* (black bars) samples were normalized to the corresponding mock-treated controls (black line). Error bars represent SD of at least three biological replicates. Asterisks indicate statistically significant differences from the mock-treated control, and plus signs indicate statistically significant differences compared with ISX-treated Col-0 sample. WT, Wild type.

ixr1-1 seedlings compared with the Col-0 controls (Supplemental Table S1).

It has been shown that manipulation of starch levels can result in the induction of senescence and the activation of genes involved in cell death (Yandeau-Nelson et al., 2011). Programmed cell death was detected in Arabidopsis suspension culture cells after 24 h of thaxtomin A and 48 h of ISX treatment (Duval et al., 2005). To determine if cell death is occurring under our experimental conditions and the time frame analyzed, Evans blue assays were performed on seedlings treated with the chemicals used in the experiments presented here and below (Supplemental Fig. S5 and Supplemental Materials and Methods S1; Sanevas et al., 2007). While the Evans blue assays did not detect enhanced levels of cell death after 10 h of CBI or polyethylene glycol (PEG) treatment, levels were enhanced in DCB-treated seedlings but still lower than the positive controls for cell death (NaCl and dimethyl sulfoxide; Supplemental Fig. S5).

To summarize, the cell viability assays show that ISX treatment does not cause large-scale cell death whereas DCB-treated seedlings do exhibit some. The effects observed with DCB were not as pronounced as with ISX. However, measurements of Rubisco activase levels, soluble sugars, and starch in mock-, DCB-, and ISX-treated Col-0 and *ixr1-1* seedlings show that CBI affects specifically Rubisco activase levels and causes a transient redistribution of carbohydrates. The reduced Rubisco activase levels in the *ixr1-1* seedlings are correlated with lower levels of soluble sugars and starch, suggesting that the carbohydrate metabolism in general might be reduced in the mutant background.

Analysis of Different Signaling Cascades Possibly Mediating the CBI-Induced Carbohydrate Redistribution

To determine if an established signaling mechanism is required to mediate the changes observed in gene expression and carbohydrate distribution, mutants impaired in different signaling cascades were used. ISX was employed for these experiments, since its effects on gene expression and metabolism are more direct than those of DCB. We tested if the ISX-induced metabolic and gene expression changes described above were modified in any of the following mutants: (1) sugar-signaling *Glc insensitive2* (*gin2-1*; Moore et al., 2003); (2) metabolic signaling *snf1 kinase homolog10* (*kin10*) and *kin11* (Baena-González et al., 2007); (3) regulation of sugar distribution *aba deficient2* (*aba2-1*; Rook et al., 2001) and *tonoplast monosaccharide transporter1-2-3* (*tmt1-2-3*; Wormit et al., 2006); (4) osmosensing *Arabidopsis His kinase1* (*ahk1*) and osmo/cytokinin-sensing *cytokinin receptor1* (*cre1*; Tran et al., 2007); (5) cell wall signaling *wall-associated kinase1* (*wak1*; Brutus et al., 2010); (6) ROS production (*rbohDF*; Kwak et al., 2003); and (7) calcium uptake during mechanoperception and regulation of cell wall damage-induced lignin production (*mca1*; Nakagawa et al., 2007; Denness et al., 2011).

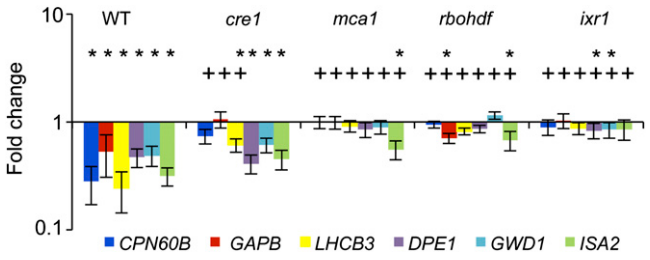

Figure 4. qRT-PCR-based expression analysis of genes involved in carbohydrate metabolism after 4 h of ISX treatment in different mutant backgrounds. Values are means ± SE from three biological replicates. Asterisks indicate statistically significant differences compared with the expression of the same gene in mock-treated samples, and plus signs indicate statistically significant differences compared with the expression of the same gene in the ISX-treated Col-0 sample. WT, Wild type.

qRT-PCR-based expression analysis showed that ISX-induced changes in transcript levels (similar to Col-0) were still detectable in *gin2*, *kin10*, *kin11*, *ahk1*, *wak1*, *tmt1-2-3*, and *aba2-1* seedlings (data not shown). In *cre1* seedlings, expression of the genes analyzed showed a reduced but still significant reduction following CBI (Fig. 4). In *mca1* and *rbohDF* seedlings, expression of most of the genes analyzed did not change in response to CBI treatment (Fig. 4), similar to the *ixr1-1* control.

In parallel, soluble sugar and starch levels were quantified in seedlings of all the mutants before treatment commenced and after 10 h of mock or ISX treatment. Several mutants (*aba2*, *kin11*, *tmt1-2-3*, *gin2*, *mca1*, *rbohDF*, and *irx1*) exhibited differences in starch levels compared with the control before the start of treatment (Supplemental Table S1). However, all the mutants analyzed exhibited enhanced starch levels upon ISX treatment compared with the corresponding mock-treated controls. These results suggest that the mechanisms mediating the changes in starch levels are not fundamentally impaired in the mutants assessed. To summarize, while the results from the expression profiling analysis implicate *MCA1*, *CRE1*, and *RBOHDF* in mediating the changes in transcript levels induced by ISX, the carbohydrate measurements showed that none of the mutations impair the ISX-induced changes in starch levels. These results suggest that either the mechanism mediating the response to ISX is redundantly organized (i.e. several signaling cascades could act in parallel) or an unknown novel signaling mechanism is mediating the ISX-induced changes in carbohydrate distribution.

CBI and Hyperosmotic Stress Treatments Induce Different Metabolic Changes

The results presented above suggested that none of the regulatory mechanisms impaired in the mutants investigated is responsible for mediating the ISX-induced metabolic changes. CBI treatment has been shown

previously to cause both the loss of the cellulose synthase complexes from the plasma membrane in root epidermal cells and the swelling of these cells (Lazzaro et al., 2003; Paredez et al., 2006; Hamann et al., 2009; Tsang et al., 2011). It seems likely that the swelling is caused by turgor pressure in the individual cell pushing against a weakened cell wall. ISX-induced effects, such as cell swelling, lignin deposition, necrosis, and gene expression changes, can be prevented by osmotic support in a concentration-dependent manner using sorbitol or mannitol (Hamann et al., 2009). Both sugar alcohols are frequently used for the analysis of hyperosmotic stress responses and the manipulation of turgor pressure in plants (Donaldson et al., 2004; Boudsocq et al., 2007). Previous work has shown that hyperosmotic stress (to simulate water stress) causes carbohydrate redistribution in potato tuber slices, with Suc levels being enhanced and starch levels decreased (Oparka and Wright, 1988a, 1988b). Therefore, we decided to investigate if ISX and hyperosmotic stress treatments result in similar effects on carbohydrate distribution. Accordingly, starch and soluble sugar levels were analyzed after seedlings were treated with ISX, 5% PEG, 300 mM sorbitol, 300 mM mannitol, 150 mM NaCl, or 150 mM KCl for 10 h (Fig. 5; Supplemental Table S2). Mannitol/sorbitol treatments result in significantly enhanced levels of Glc and Fru, while Suc and starch levels are reduced (Fig. 5, dark gray and dark gray hatched bars). NaCl- and KCl-treated seedlings exhibit decreases in the levels of Glc, Fru, and starch, while the Suc levels are increased (Fig. 5, light gray and light gray hatched bars). Only the starch levels were significantly reduced in 5% PEG-treated seedlings (Fig. 5, white bars). The soluble sugars did not exhibit significant differences. Interestingly, ISX-treated seedlings exhibit lower Glc, Fru, and Suc levels than any of the other treatments investigated and are the only seedlings that exhibit increased starch levels compared with the mock-treated controls (Fig. 5, black bars).

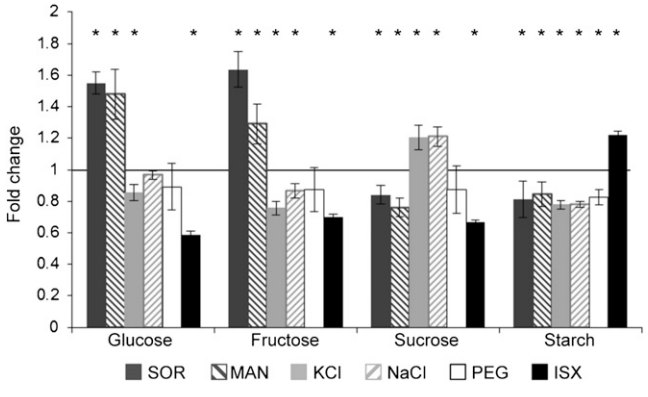

Figure 5. Comparison of metabolic effects caused by ISX and hyperosmotic treatments in Arabidopsis seedlings. Sugar and starch contents are shown for Col-0 seedlings after 300 mM sorbitol, 300 mM mannitol, 150 mM KCl, 150 mM NaCl, 5% PEG, or ISX treatment for 10 h. Data were normalized to the mock-treated Col-0 sample (black line). Asterisks indicate statistically significant differences compared with the mock-treated Col-0 sample. Error bars represent SD of three biological replicates.

These results suggest that ISX treatment has a different effect on carbohydrate distribution than osmotica used to generate hyperosmotic shocks, particularly regarding starch levels. The increased levels of Glc and Fru in mannitol/sorbitol-treated seedlings suggest that sorbitol/mannitol could be stronger osmotica or support previous observations that these sugar alcohols might be metabolized by plants, thus possibly influencing primary metabolism (Loescher, 1987). NaCl/KCl induce changes in soluble sugar and starch levels, but they have side effects due to their ionic character. Therefore, they are more suitable to simulate salt stress instead of osmotic stress. PEG treatment is possibly the best method to provide osmotic support/manipulate turgor pressure, because PEG neither has an ionic characteristic nor can it be metabolized (Kaufmann and Eckard, 1971; Michel and Kaufmann, 1973).

Osmotic Support Neutralizes the CBI Effects on Gene Expression and Carbohydrate Distribution

The results presented in Figure 5 suggested that CBI has a different effect on carbohydrate distribution than hyperosmotic stress treatments. We have previously shown that osmotic support (hyperosmotic stress treatment) suppresses the effects of ISX treatment on seedling morphology and gene expression levels (Hamann et al., 2009). Taken together, these results raise the possibility that changes in turgor pressure may either affect the same processes or be responsible for the observed effects caused by CBI.

To follow up on these observations, seedlings were treated with ISX or DCB alone or in combination with 5%/10% PEG or 300 mM sorbitol (as a control), and the impacts of the treatments on both gene expression and soluble sugar/starch levels were determined. Gene expression levels were not affected by 5% PEG treatment alone (Supplemental Fig. S6B) and were reduced by both ISX and DCB (Fig. 6A; Supplemental Fig. S6B). Combining ISX treatment with 5%/10% PEG or 300 mM sorbitol reduced the impact of ISX on gene expression (Fig. 6A, 5%/10% PEG; Supplemental Fig. S6A, 300 mM sorbitol). Combining DCB treatments with 5% PEG had a similar but not as pronounced effect (Supplemental Fig. S6B).

To examine if combining PEG with ISX also affects CBI-induced carbohydrate redistribution, soluble sugars and starch contents were measured in seedlings treated with/without ISX and three different PEG concentrations (2.5%, 5%, and 10%). Increasing concentrations of PEG in samples without ISX had very limited effects on carbohydrate levels (Supplemental Fig. S7A). In control (no-PEG) CBI-treated seedlings, decreases in Glc, Fru, and Suc levels were observed, whereas starch content was enhanced (Fig. 6B, black

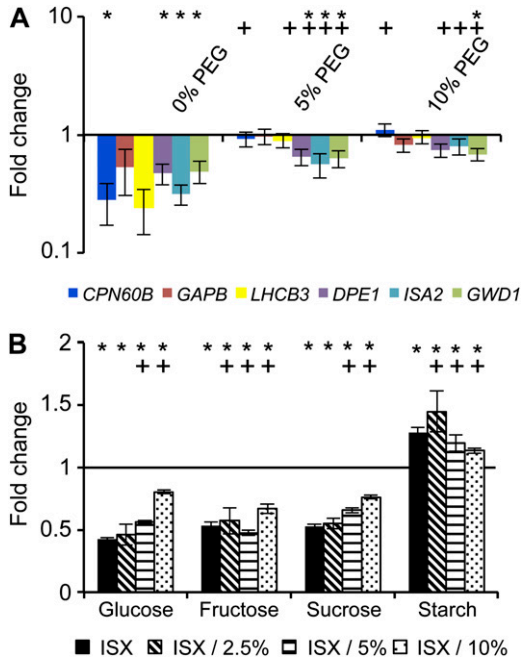

Figure 6. Effects of osmotic support on CBI-induced changes in gene expression and carbohydrate levels A, qRT-PCR expression analysis of genes involved in photosynthesis and starch metabolism after ISX (0% PEG), ISX/5% PEG and ISX/10% PEG treatment. Values are means ± SE from three biological replicates. B, Sugar and starch contents of Col-0 seedlings treated with ISX alone, with ISX/2.5% PEG, with ISX/5% PEG, or with ISX/10% PEG. Data were normalized to the mock-treated Col-0 sample without PEG (black line). Asterisks indicate statistically significant differences compared with the mock-treated sample, and plus signs indicate statistically significant differences compared with the ISX-treated sample. Samples in A were treated for 4 h, and those in B for 10 h.

bars). PEG treatment did not affect CBI-induced Fru changes in a concentration-dependent manner. However, the addition of PEG reduced the CBI effect on Glc, Suc, and starch levels in a concentration-dependent manner (Fig. 6B; Supplemental Table S2). To confirm the specificity of the observed effects, seedlings were also treated with a combination of ISX and sorbitol (Supplemental Fig. S7B) or DCB and PEG (Supplemental Fig. S7C). Sorbitol treatment by itself affected carbohydrate distribution as described previously and reduced the effect of ISX on starch accumulation (Supplemental Fig. S7B). Similarly, while DCB-treated seedlings exhibited increased starch levels, cotreatment with PEG reduced the starch levels (Supplemental Fig. S7C). It was also determined whether turgor pressure manipulation neutralizes the CBI-induced reduction of Rubisco activase levels, so enzyme levels were determined in seedlings mock, PEG, ISX, DCB, ISX/PEG, or DCB/PEG treated. No reproducible effects of osmotic support on Rubisco activase levels were detectable (data not shown).

To summarize, the results show that the CBI-induced effects on the expression of genes involved in starch metabolism and photosynthesis can be suppressed by osmotic support. Combining different osmotica (sorbitol and PEG) with different inhibitors (ISX and DCB) reduces the effects of CBI treatment on starch levels in a concentration-dependent manner. These results show that changes in carbohydrate distribution induced by CBI can be reduced/neutralized by providing osmotic support.

CRE1, *MCA1*, and *RBOHDF* Are Involved in the Suppression of CBI Effects by Osmotic Support

To identify the signaling cascades mediating the effects of osmotic support on carbohydrate metabolism, the same mutants as described above were employed. It was determined whether osmotic support (by PEG) still prevents the ISX-induced reduction in transcript levels and changes in carbohydrate distribution in the different mutant backgrounds.

qRT-PCR-based expression analysis found that in *ixr1-1* seedlings (included as a positive control), the expression of *CPN60B* and *GWD1* was slightly increased after 4 h of 5% PEG/ISX treatment. The expression analysis showed that osmotic support reduced the CBI-induced expression effects in *gin2*, *kin10*, *kin11*, *ahk1*, *wak1*, *tmt1-2-3*, and *aba2-1* seedlings similar to the Col-0 control, suggesting that these genes are not involved in the process examined (data not shown). Interestingly, in ISX/PEG-treated *rbohDF* and *cre1* seedlings, the expression levels of the genes examined were less affected by PEG treatment than in the control (Fig. 7A). The levels of gene expression in 5% PEG/ISX-treated *mca1* seedlings were very similar to those of mock-treated controls (compare Figs. 7A and 4).

Soluble sugar and starch levels were measured in Col-0, *cre1*, *mca1*, and *rbohDF* seedlings treated with 5% PEG and ISX for 10 h (Fig. 7B; Supplemental Table S1). Increased starch levels were detected upon ISX treatment in Col-0, *cre1*, *mca1*, and *rbohDF* seedlings but not in *ixr1-1* (Fig. 7B, black bars). In Col-0 and *mca1* seedlings treated with PEG, reduced starch levels were detected compared with the corresponding mock controls (Fig. 7B, light gray hatched bars). Starch levels were slightly enhanced in *ixr1-1* seedlings while being similar to the corresponding controls in *cre1* and *rbohDF*, suggesting that both mutants are impaired in the detection of PEG in the medium. No significant increase in starch levels was detected in Col-0 seedlings upon PEG/ISX cotreatment (Fig. 7B, black hatched bar, highlighted by the red arrow). Starch levels were slightly reduced compared with the control in *ixr1-1* seedlings. In PEG/CBI-treated *cre1*, *mca1*, and *rbohDF* seedlings, the starch levels were increased, which differed from the corresponding Col-0 control (red arrow). This suggests that MCA1, CRE1, and RBOHDF are required for the PEG-based suppression of ISX-induced changes. To summarize, PEG-based suppression of the ISX-induced changes in gene expression and starch levels is reduced in *cre1* and

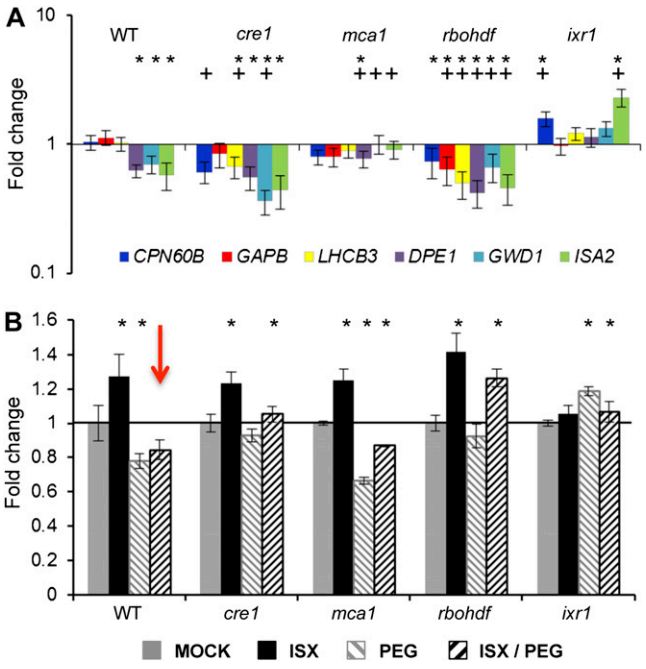

Figure 7. Functional characterization of genes mediating the osmotic support-induced suppression of ISX treatment. A, qRT-PCR-based expression analysis of genes involved in carbohydrate metabolism after 4 h of ISX/5% PEG treatment in Col-0 and mutant seedlings. Values are means ± SE from three biological replicates. Asterisks indicate statistically significant differences compared with the expression of the same gene in mock-treated samples, and plus signs indicate statistically significant differences compared with the expression of the same gene in 5% PEG/ISX-treated Col-0 samples. B, Starch levels in Col-0 and mutant seedlings mock, ISX, 5% PEG, or ISX/5% PEG treated for 10 h. The red arrow highlights the starch content in ISX/5% PEG-treated Col-0 seedlings. Data were normalized to the corresponding mock-treated control without PEG (black line). Values are means ± SD from three biological replicates. Asterisks indicate statistically significant differences compared with the corresponding mock-treated samples. WT, Wild type.

rbohDF seedlings. In *mca1* seedlings, the gene expression levels are similar to ISX treatment alone but the PEG-based suppression of changes in starch levels is not detectable. These observations suggest that the turgor-sensitive suppression of ISX-induced metabolic changes is mediated by *CRE1*, *RBOHDF*, and *MCA1* and is based on a mechanism separate from ISX perception/response.

DISCUSSION

The coordination of photosynthetic activity with primary metabolism and the redistribution of carbohydrates in response to abiotic and biotic stress in plants has been discussed previously (Paul and Foyer, 2001). Soluble sugar levels have been identified as integrating elements linking plant metabolism and the environment, since they are influenced both by sink activities and biotic/abiotic stresses (Geigenberger, 2011).

In order to determine how the activities of cellulose biosynthesis, primary metabolism, and photosynthesis are coordinated, we inhibited cellulose biosynthesis using two inhibitors (ISX and DCB) with distinctly different modes of action. Overall, the results obtained with both were similar. However, DCB seems not to be such an effective inhibitor, based on the delayed (changes in gene expression levels) and less pronounced (changes in soluble sugars and starch levels) responses of Arabidopsis seedlings to the inhibitor treatment. In addition, DCB-treated seedlings exhibited elevated levels of cell death. We found that both mock- and CBI-treated seedlings exhibit an initial increase in Suc (probably from the fresh medium provided) at the start of treatment. While the mock-treated seedlings then show transient increases in Glc/Fru levels and no change in starch, CBI treatment results in a transient increase in starch levels but no increases in Glc and Fru. Increased starch contents upon CBI have been observed previously in the temperature-sensitive Arabidopsis mutants *radially swollen1*, *-2*, and *-3* (Peng et al., 2000). Conversely, reduced starch levels and thicker cell walls have been described in leaves of the pea (*Pisum sativum*) mutant *rugosus3*, which is impaired in the plastidial phosphoglucomutase (Harrison, 1998). These observations suggest that a dedicated regulatory mechanism coordinates starch and cellulose biosynthesis, that they may compete for the same carbon source, and that reduction in one activity leads to enhancement in the other. This hypothesis is supported by the negative correlation observed between biomass production/growth and starch levels across 94 Arabidopsis accessions (Sulpice et al., 2009).

Photosynthetic activity is partially sink regulated, and soluble sugar levels can regulate enzyme activities and the expression of genes involved in primary metabolism and photosynthesis (Koch, 1996; Gupta and Kaur, 2005). High sugar levels cause increased starch synthesis, reductions of transcript levels of genes involved in photosynthesis, and the inhibition of photosynthetic activity (Koch, 1996; Geigenberger et al., 2005). Here, we found that CBI reduced the expression of genes involved in photosynthesis and, in the case of ISX, also reduced Rubisco activase levels, although the soluble sugar levels were lower in inhibitor-treated seedlings than in mock controls. Rubisco activase is required for the activation of Rubisco in vivo, and it was shown that activase deficiency leads to decreased PSII activity (Cai et al., 2010; Carmo-Silva and Salvucci, 2011). These results show that the expression of genes involved in carbohydrate metabolism and Rubisco activase/photosynthesis can be inhibited in the absence of high levels of soluble sugars. The data suggest that another mechanism may exist that can regulate the expression of genes involved in carbohydrate metabolism and Rubisco activase levels.

To gain insights into the mode of action of the mechanism regulating the observed CBI-induced metabolic

and gene expression effects, mutants impaired in different signaling pathways were systematically tested. For these experiments, only ISX was used, since the available evidence suggests that it is more specific than DCB. The metabolic and gene expression changes detected in *gin2*, *kin10*, *kin11*, *ahk1*, *wak1*, *tmt1-2-3*, and *aba2-1* seedlings to treatments were similar to the Col-0 control, suggesting that the signaling cascades impaired in these mutants are not involved in the processes examined here. In *mca1*, *cre1*, and *rbohDF* seedlings, ISX-induced expression changes were absent but starch levels were still enhanced. Previous work has shown that these three genes are required for CBI-induced lignin deposition (Denness et al., 2011). Therefore, these results suggest that a distinct mechanism is responsible for mediating the CBI-induced changes in carbohydrate distribution.

Previous results from our own and other research groups have shown that the manipulation of turgor pressure suppresses CBI-induced lignin production in Arabidopsis seedlings and modifies Suc and starch levels in potato tuber slices (Oparka and Wright, 1988a, 1988b; Chaves, 1991; Geigenberger et al., 1999a, 1999b; Hamann et al., 2009; Valerio et al., 2011). Here, we compared the effects of different osmotica (normally used to create hyperosmotic stress) and CBI on soluble sugar and starch levels. The results suggest that CBI has distinctly different effects on carbohydrate levels compared with mannitol, sorbitol, NaCl, KCl, and PEG. In particular, starch levels in CBI-treated seedlings were enhanced, which was not the case in seedlings exposed to hyperosmotic stress conditions. The combination of hyperosmotic stress (caused by PEG or sorbitol) with CBI treatments led to the suppression of CBI-induced gene expression changes and reduction of the CBI-induced redistribution of carbohydrates. These results suggest that the CBI-induced effects may be responsive to changes in turgor pressure and that CBI may have opposite effects on turgor pressure compared with hyperosmotic treatments. Loosening of the plant cell wall due to CBI could allow cell expansion, which in turn could affect turgor pressure. Bulging epidermal cells in CBI-treated seedlings have been described before and would support this hypothesis (Hamann et al., 2009; Tsang et al., 2011). Previous work by other research groups has provided additional evidence for the importance of plant cell walls in the regulation of turgor pressure and response to drought/osmotic stress (Zhu et al., 1993, 2010; Chen et al., 2005). To summarize, the results presented here suggest that a turgor pressure-sensitive mechanism could regulate carbohydrate metabolism and raise the question of whether CBI treatment could generate a hypoosmotic stress situation (since hyperosmotic stress treatments have been shown to suppress the CBI-induced changes in transcript and enhanced starch levels).

In Col-0 seedlings, combining CBI and PEG treatments resulted in suppression of the inhibitor-induced gene expression changes and metabolic effects. In *mca1*, *cre1*, and *rbohDF* seedlings, osmotic support did not suppress the CBI effects on starch levels. By contrast, transcript levels were slightly reduced in CBI/PEG-treated *cre1* and *rbohdf* seedlings and not significantly changed in *mca1* seedlings. Since there are no differences regarding transcript levels detectable between CBI and CBI/PEG treatment in *mca1* seedlings, the exact role of MCA1 in this context would be difficult to characterize if only gene expression data were being considered. However, the data from the starch quantifications in the three mutants suggest that all three genes are required for the osmotic suppression of CBI-induced starch changes. *CRE1* has been shown to function as a cytokinin receptor in plants, to be able to rescue an osmosensor (*SLN1*)-deficient yeast strain in the presence of cytokinin, and has been implicated in the ABA-mediated response to drought stress (Inoue et al., 2001; Reiser et al., 2003; Tran et al., 2007). Previous research has shown that CBI causes no increases in ABA levels in liquid culture-grown seedlings and that genes involved in ABA metabolism/signaling do not exhibit dramatic changes in transcript levels (Hamann et al., 2009; A. Wormit, unpublished data). In parallel, cytokinin-deficient mutant seedlings exhibit the same response to CBI as the Col-0 seedlings (A. Wormit, unpublished data). *RBOHD* and *RBOHF* encode NADPH oxidase enzymes that are required to generate ROS during the response to biotic and abiotic stress (Torres et al., 2002). Mild salt stress results in the activation of *RBOHD* expression and increased ROS production, whereas overexpression of a *Chlamydomonas* glutathione peroxidase improves salt stress tolerance in tobacco (*Nicotiana tabacum*) plants (Yoshimura et al., 2004; Xie et al., 2011). Characterization of the *salt-overly sensitive6* allele of *ARABIDOPSIS CELLULOSE SYNTHASE-LIKE D5* has implicated ROS-based signaling processes in the response to osmotic stress (Zhu et al., 2010). *MCA1* encodes a plasma membrane protein that can partially rescue a yeast strain deficient in the MID1 CCH1 stretch-activated calcium channel (Nakagawa et al., 2007). *MCA1* has been implicated in Ca^{2+} signaling, mechanosensing in Arabidopsis roots, and CBI-induced lignin deposition (Nakagawa et al., 2007; Hamann et al., 2009). These results suggest that RBOHDF, MCA1, and CRE1 could perceive changes in turgor pressure and/or plasma membrane distortion caused by turgor manipulation. *cre1* and *rbohDF* seedlings do not exhibit reductions in starch levels like the Col-0 control upon PEG treatment, suggesting that they are fundamentally impaired in the perception of turgor pressure changes. *mca1* seedlings exhibit a more pronounced reduction in starch levels upon PEG treatment alone, suggesting that they are hypersensitive to turgor manipulation and might respond to a different stimulus. This situation could be similar to that in yeast cells, where osmoperception (SLN1), stretch-activated calcium channels (MID1 CCH1), and cell wall integrity monitoring pathways perceive different inputs but interact to generate a

response tailored to a particular stimulus (García et al., 2009). The translation of signals in plants generated by CRE1 and MCA1 could occur via RBOHDF-derived ROS, since the activity of the enzyme is regulated synergistically by phosphorylation and Ca^{2+} influx (Cazalé et al., 1998; Ogasawara et al., 2008). Since the mutants affect only the osmosensitive effects and not the ISX-induced starch changes, the observed metabolic effects of ISX treatment are either mediated by a redundantly specified mechanism or by another mechanism coordinating cellulose biosynthesis directly with primary metabolism and photosynthesis.

We have shown here that changes in the activity of cellulose biosynthesis reduce the expression of genes involved in starch degradation and photosynthesis, that the changes cause a redistribution of carbohydrates, and that they reduce the levels of Rubisco activase in Arabidopsis seedlings. In addition, we have shown that manipulation of turgor pressure can suppress the CBI effects on gene expression and carbohydrate distribution in a concentration-dependent manner. *CRE1*, *MCA1*, and *RBOHDF* are essential for the osmosensitive responses but not the ones induced by ISX. These results suggest that two different signaling mechanisms exist. The first coordinates the activity of cellulose biosynthesis with primary metabolism and photosynthesis. The second is a turgor pressure-sensitive mechanism that can modify carbohydrate metabolism. The latter raises the possibility that turgor pressure could act as a central integrator enabling the plant cell to monitor and coordinate different metabolic and cellular processes in response to both environmental and cellular stimuli.

MATERIALS AND METHODS

Plant Material

Arabidopsis (*Arabidopsis thaliana*) wild-type (Col-0) and mutant seedlings were grown and treated with 600 nM ISX as described (Hamann et al., 2009). For combined treatments, the respective PEG 8000, sorbitol, and mannitol amounts were dissolved in the growth medium. All chemicals were obtained from Sigma unless stated otherwise. Mutants were obtained from the Nottingham Arabidopsis Stock Center (Arabidopsis.info/) or from specific laboratories: *cre1-10* (*At2g01830*), *mca1* (*At4g35920*), *rbohDF* (J.J. Jones, Sainsbury Laboratory; *At5g47910*, *At1g64060*), *gin2_1* (*At4g29130*), *aba2_1* (*At1g52340*), *kin10* (SALK_127939.21.55.x, *At3g01090*), *kin11* (WiscDsLox320B03, *At3g29160*), *ahk1* (SALK_000977.28.80.x, *At2g17820*), *wak1* (B.K. Kohorn, Bowdoin College), and *tmt1-2-3* (E.N. Neuhaus, University of Kaiserslautern).

qRT-PCR

For RNA isolation, the RNAeasy Mini Kit was used according to the manufacturer's protocol (http://www.qiagen.com). For cDNA synthesis, the Qiagen QuantiTect Rev. Transcription Kit was used as described by the manufacturer. The Qiagen QuantiTect SYBR Green PCR Kit was used to perform qRT-PCR expression analysis on a Corbett Rotorgene 3000 machine according to the manufacturer's instructions (http://corbettlifescience.com) and an Applied Biosystems 7500 PCR system. The sequence of qRT-PCR primers used is listed in Supplemental Materials and Methods S1. For data analysis, Relative Expression Software Tool 384, version 2 (Pfaffl et al., 2002) was used. Expression data were standardized using *UBIQUITIN10* and normalized to the expression of the respective gene in mock-treated samples.

Carbohydrate Measurement

Plant tissue samples were freeze dried and then ground to a fine powder using a TissueLyser (Qiagen) with metal steel balls (25 Hz, 2 min). Soluble sugars were extracted in successive aliquots of 80% ethanol at 95°C. Ethanol fractions were pooled, and the released Glc, Fru, and Suc were analyzed sequentially using a coupled enzymatic assay. In this assay, the reduction of $NADP^+$ is directly proportional to the substrate concentration and was determined spectrophotometrically at an optical density at 340 nm (Jones et al., 1977; Passonneau and Lowry, 1993). The residual tissue material was used for starch extraction as described (Reinhold et al., 2007). After hydrolysis, starch was quantified as Glc units as described above. The soluble sugar and starch contents were calculated as averages ± SD of at least three biological replicates, and each experiment was repeated at least three times.

Metabolic Flux Measurement

Arabidopsis seedlings were grown and treated with ISX as described (Hamann et al., 2009). Radiolabel (30 mM Suc at a specific activity of 2.1 MBq $mmol^{-1}$) was added at three different time points: 1 h before the CBI treatment or 7 or 11 h after the treatment commenced. Following the provision of radiolabel, incubations were continued for 1 h, then plant material was harvested, washed three times in half-strength Murashige and Skoog medium in 2.56 mM MES buffer (100 mL per sample), and frozen in liquid nitrogen.

Plant material was extracted with 80% (v/v) ethanol at 80°C (1 mL per sample) and reextracted in two subsequent steps with 50% (v/v) ethanol; the combined supernatants were dried under an air stream at 40°C and taken up in 1 mL of water. Label was separated by ion-exchange chromatography and thin-layer chromatography as described (Fernie et al., 2001). Insoluble material remaining after ethanol extraction was analyzed for label in starch, cell wall, and protein as described (Fernie et al., 2002). Absolute fluxes were calculated from the label incorporation divided by the specific activity of the hexose phosphate pools in the samples (Geigenberger et al., 2005). For flux to glycolysis, the sum of label retained in protein, amino acids, organic acids, and released $^{14}CO_2$ was determined. The specific activity was calculated by dividing the label incorporation in the hexose phosphate pool by the absolute levels of hexose phosphates.

Measurement of Relative Rubisco Activase Levels

Arabidopsis seedlings were harvested and flash frozen in liquid nitrogen. Frozen seedlings were homogenized and resuspended in ice-cold extraction buffer (100 mg mL^{-1}; 50 mM HEPES, pH 7.5, with KOH, 20% [v/v] glycerol, 0.25% [w/v] bovine serum albumin, 1% [v/v] Triton X-100, 10 mM $MgCl_2$, 1 mM EDTA, 1 mM EGTA, 0.5 mM dithiothreitol, and Sigma Plant Protease Inhibitor Cocktail), as adapted from Sulpice et al. (2007). The mixture was vortexed and centrifuged for 10 min at 0°C. Relative Rubisco activase amount was measured using an ELISA (Sigma) adapted for these experiments. Briefly, seedling extracts were diluted in carbonate-bicarbonate buffer supplemented with fresh protease inhibitors (final concentration of 0.5 mg fresh weight mL^{-1}). Proteins (200 μL of the diluted cell mixture) were allowed to bind to the surface of the microplate wells (Costar high bind) for 45 min at 37°C. Wells were washed (phosphate-buffered saline containing 0.05% Tween 20), blocked (5% bovine serum albumin in phosphate-buffered saline; 2 h at room temperature), and washed again. Bound Rubisco activase was determined using goat anti-Rubisco activase antibodies (Santa Cruz) and donkey anti-goat antibodies conjugated with horseradish peroxidase (Sigma). Horseradish peroxidase activity was detected using Lumi-Light substrate (Roche). Unspecific binding was accounted for by deducting a buffer-only control containing no protein, and absorbance was measured at 450 nm in a Thermo Scientific multiwell microplate reader.

Statistical Analysis

Unless stated otherwise in the figure legends, statistical tests were performed as follows. Comparisons of the saccharide contents were based on three data points. In both cases, a one-way ANOVA with a two-tailed distribution and a 0.05 degree of significance was performed. qRT-PCR results were compared using eight individual data points with a one-way ANOVA, a two-tailed distribution, and a 0.01 degree of significance.

Supplemental Data

The following materials are available in the online version of this article.

Supplemental Figure S1. Microarray-based expression profiling of ISX-treated Arabidopsis seedlings.

Supplemental Figure S2. qRT-PCR-based expression profiling of DCB-treated Arabidopsis seedlings.

Supplemental Figure S3. Metabolic flux measurements of ISX-treated Arabidopsis seedlings.

Supplemental Figure S4. Quantification of soluble sugars and starch levels in DCB-treated Arabidopsis seedlings.

Supplemental Figure S5. Results of Evans blue assays of Arabidopsis seedlings.

Supplemental Figure S6. qRT-PCR based expression profiling of Arabidopsis seedlings treated with osmotica and/or inhibitors.

Supplemental Figure S7. Soluble sugars and starch levels in PEG-treated Arabidopsis seedlings.

Supplemental Table S1. Starch and soluble sugar levels Col-0 and mutant seedlings.

Supplemental Table S2. Effects of osmotica on soluble sugar and starch levels in Col-0 seedlings.

Supplemental Table S3. Rubisco activase levels in Col-0 seedlings.

Supplemental Materials and Methods S1. Absolute soluble sugar/starch levels and assay details.

Received February 6, 2012; accepted March 14, 2012; published March 15, 2012.

LITERATURE CITED

Baena-González E, Rolland F, Thevelein JM, Sheen J (2007) A central integrator of transcription networks in plant stress and energy signalling. Nature **448:** 938–942

Bläsing OE, Gibon Y, Günther M, Höhne M, Morcuende R, Osuna D, Thimm O, Usadel B, Scheible WR, Stitt M (2005) Sugars and circadian regulation make major contributions to the global regulation of diurnal gene expression in *Arabidopsis*. Plant Cell **17:** 3257–3281

Boudsocq M, Droillard MJ, Barbier-Brygoo H, Laurière C (2007) Different phosphorylation mechanisms are involved in the activation of sucrose non-fermenting 1 related protein kinases 2 by osmotic stresses and abscisic acid. Plant Mol Biol **63:** 491–503

Brutus A, Sicilia F, Macone A, Cervone F, De Lorenzo G (2010) A domain swap approach reveals a role of the plant wall-associated kinase 1 (WAK1) as a receptor of oligogalacturonides. Proc Natl Acad Sci USA **107:** 9452–9457

Cai B, Zhang A, Yang Z, Lu Q, Wen X, Lu C (2010) Characterization of photosystem II photochemistry in transgenic tobacco plants with lowered Rubisco activase content. J Plant Physiol **167:** 1457–1465

Carmo-Silva AE, Salvucci ME (2011) The activity of Rubisco's molecular chaperone, Rubisco activase, in leaf extracts. Photosynth Res **108:** 143–155

Cazalé AC, Rouet-Mayer MA, Barbier-Brygoo H, Mathieu Y, Laurière C (1998) Oxidative burst and hypoosmotic stress in tobacco cell suspensions. Plant Physiol **116:** 659–669

Chaves MM (1991) Effects of water deficits on carbon assimilation. J Exp Bot **42:** 1–16

Chen ZZ, Hong XH, Zhang HR, Wang YQ, Li X, Zhu JK, Gong ZZ (2005) Disruption of the cellulose synthase gene, AtCesA8/IRX1, enhances drought and osmotic stress tolerance in Arabidopsis. Plant J **43:** 273–283

Coleman HD, Samuels AL, Guy RD, Mansfield SD (2008) Perturbed lignification impacts tree growth in hybrid poplar: a function of sink strength, vascular integrity, and photosynthetic assimilation. Plant Physiol **148:** 1229–1237

Delmer DP (1999) Cellulose biosynthesis: exciting times for a difficult field of study. Annu Rev Plant Physiol Plant Mol Biol **50:** 245–276

Demura T, Ye ZH (2010) Regulation of plant biomass production. Curr Opin Plant Biol **13:** 299–304

Denness L, McKenna JF, Segonzac C, Wormit A, Madhou P, Bennett M, Mansfield J, Zipfel C, Hamann T (2011) Cell wall damage-induced lignin biosynthesis is regulated by a reactive oxygen species- and jasmonic acid-dependent process in Arabidopsis. Plant Physiol **156:** 1364–1374

Desprez T, Vernhettes S, Fagard M, Refrégier G, Desnos T, Aletti E, Py N, Pelletier S, Höfte H (2002) Resistance against herbicide isoxaben and cellulose deficiency caused by distinct mutations in same cellulose synthase isoform CESA6. Plant Physiol **128:** 482–490

Donaldson L, Ludidi N, Knight MR, Gehring C, Denby K (2004) Salt and osmotic stress cause rapid increases in Arabidopsis thaliana cGMP levels. FEBS Lett **569:** 317–320

Duval I, Brochu V, Simard M, Beaulieu C, Beaudoin N (2005) Thaxtomin A induces programmed cell death in Arabidopsis thaliana suspension-cultured cells. Planta **222:** 820–831

Fernie AR, Roscher A, Ratcliffe RG, Kruger NJ (2001) Fructose 2,6-bisphosphate activates pyrophosphate:fructose-6-phosphate 1-phosphotransferase and increases triose phosphate to hexose phosphate cycling in heterotrophic cells. Planta **212:** 250–263

Fernie AR, Roscher A, Ratcliffe RG, Kruger NJ (2002) Activation of pyrophosphate:fructose-6-phosphate 1-phosphotransferase by fructose 2,6-bisphosphate stimulates conversion of hexose phosphates to triose phosphates but does not influence accumulation of carbohydrates in phosphate-deficient tobacco cells. Physiol Plant **114:** 172–181

Fischer M, Schnell N, Chattaway J, Davies P, Dixon G, Sanders D (1997) The Saccharomyces cerevisiae CCH1 gene is involved in calcium influx and mating. FEBS Lett **419:** 259–262

García R, Rodríguez-Peña JM, Bermejo C, Nombela C, Arroyo J (2009) The high osmotic response and cell wall integrity pathways cooperate to regulate transcriptional responses to zymolyase-induced cell wall stress in Saccharomyces cerevisiae. J Biol Chem **284:** 10901–10911

Geigenberger P (2011) Regulation of starch biosynthesis in response to a fluctuating environment. Plant Physiol **155:** 1566–1577

Geigenberger P, Muller-Rober B, Stitt M (1999a) Contribution of adenosine 5′-diphosphoglucose pyrophosphorylase to the control of starch synthesis is decreased by water stress in growing potato tubers. Planta **209:** 338–345

Geigenberger P, Regierer B, Nunes-Nesi A, Leisse A, Urbanczyk-Wochniak E, Springer F, van Dongen JT, Kossmann J, Fernie AR (2005) Inhibition of de novo pyrimidine synthesis in growing potato tubers leads to a compensatory stimulation of the pyrimidine salvage pathway and a subsequent increase in biosynthetic performance. Plant Cell **17:** 2077–2088

Geigenberger P, Reimholz R, Deiting U, Sonnewald U, Stitt M (1999b) Decreased expression of sucrose phosphate synthase strongly inhibits the water stress-induced synthesis of sucrose in growing potato tubers. Plant J **19:** 119–129

Ghosh HP, Preiss J (1966) Adenosine diphosphate glucose pyrophosphorylase: a regulatory enzyme in the biosynthesis of starch in spinach leaf chloroplasts. J Biol Chem **241:** 4491–4504

Gupta AK, Kaur N (2005) Sugar signalling and gene expression in relation to carbohydrate metabolism under abiotic stresses in plants. J Biosci **30:** 761–776

Hamann T, Bennett M, Mansfield J, Somerville C (2009) Identification of cell-wall stress as a hexose-dependent and osmosensitive regulator of plant responses. Plant J **57:** 1015–1026

Hancock JE, Loya WM, Giardina CP, Li L, Chiang VL, Pregitzer KS (2007) Plant growth, biomass partitioning and soil carbon formation in response to altered lignin biosynthesis in Populus tremuloides. New Phytol **173:** 732–742

Harrison CJ, Hedley CL, Wang TL (1998) Evidence that the *rug3* locus of pea (*Pisum sativum* L.) encodes plastidial phosphoglucomutase confirms that the imported substrate for starch synthesis in pea amyloplasts is glucose-6-phosphate. Plant J **13:** 753–762

Hématy K, Sado PE, Van Tuinen A, Rochange S, Desnos T, Balzergue S, Pelletier S, Renou JP, Höfte H (2007) A receptor-like kinase mediates the response of Arabidopsis cells to the inhibition of cellulose synthesis. Curr Biol **17:** 922–931

Hey SJ, Byrne E, Halford NG (2010) The interface between metabolic and stress signalling. Ann Bot (Lond) **105:** 197–203

Himmelspach R, Williamson RE, Wasteneys GO (2003) Cellulose microfibril alignment recovers from DCB-induced disruption despite microtubule disorganization. Plant J **36:** 565–575

Inoue T, Higuchi M, Hashimoto Y, Seki M, Kobayashi M, Kato T, Tabata S, Shinozaki K, Kakimoto T (2001) Identification of CRE1 as a cytokinin receptor from Arabidopsis. Nature **409:** 1060–1063

Jones MG, Outlaw WH, Lowry OH (1977) Enzymic assay of 10^{-7} to 10^{-14} moles of sucrose in plant tissues. Plant Physiol **60:** 379–383

Kaufmann MR, Eckard AN (1971) Evaluation of water stress control with polyethylene glycols by analysis of guttation. Plant Physiol **47:** 453–456

Kempa S, Krasensky J, Dal Santo S, Kopka J, Jonak C (2008) A central role of abscisic acid in stress-regulated carbohydrate metabolism. PLoS ONE **3:** e3935

Kempa S, Rozhon W, Samaj J, Erban A, Baluska F, Becker T, Haselmayer J, Schleiff E, Kopka J, Hirt H, et al (2007) A plastid-localized glycogen synthase kinase 3 modulates stress tolerance and carbohydrate metabolism. Plant J **49:** 1076–1090

Kloosterman B, De Koeyer D, Griffiths R, Flinn B, Steuernagel B, Scholz U, Sonnewald S, Sonnewald U, Bryan GJ, Prat S, et al (2008) Genes driving potato tuber initiation and growth: identification based on transcriptional changes using the POCI array. Funct Integr Genomics **8:** 329–340

Koch KE (1996) Carbohydrate-modulated gene expression in plants. Annu Rev Plant Physiol Plant Mol Biol **47:** 509–540

Kwak JM, Mori IC, Pei ZM, Leonhardt N, Torres MA, Dangl JL, Bloom RE, Bodde S, Jones JD, Schroeder JI (2003) NADPH oxidase AtrbohD and AtrbohF genes function in ROS-dependent ABA signaling in Arabidopsis. EMBO J **22:** 2623–2633

Lazzaro MD, Donohue JM, Soodavar FM (2003) Disruption of cellulose synthesis by isoxaben causes tip swelling and disorganizes cortical microtubules in elongating conifer pollen tubes. Protoplasma **220:** 201–207

Levin DE (2005) Cell wall integrity signaling in Saccharomyces cerevisiae. Microbiol Mol Biol Rev **69:** 262–291

Loescher WH (1987) Physiology and metabolism of sugar alcohols in higher plants. Physiol Plant **70:** 553–557

Lu JM, Deschenes RJ, Fassler JS (2003) Saccharomyces cerevisiae histidine phosphotransferase Ypd1p shuttles between the nucleus and cytoplasm for SLN1-dependent phosphorylation of Ssk1p and Skn7p. Eukaryot Cell **2:** 1304–1314

Mangelsen E, Wanke D, Kilian J, Sundberg E, Harter K, Jansson C (2010) Significance of light, sugar, and amino acid supply for diurnal gene regulation in developing barley caryopses. Plant Physiol **153:** 14–33

Michel BE, Kaufmann MR (1973) The osmotic potential of polyethylene glycol 6000. Plant Physiol **51:** 914–916

Mikkelsen RMK, Mutenda KE, Mant A, Schürmann P, Blennow A (2005) Alpha-glucan, water dikinase (GWD): a plastidic enzyme with redox-regulated and coordinated catalytic activity and binding affinity. Proc Natl Acad Sci USA **102:** 1785–1790

Moore B, Zhou L, Rolland F, Hall Q, Cheng WH, Liu YX, Hwang I, Jones T, Sheen J (2003) Role of the Arabidopsis glucose sensor HXK1 in nutrient, light, and hormonal signaling. Science **300:** 332–336

Nakagawa Y, Katagiri T, Shinozaki K, Qi Z, Tatsumi H, Furuichi T, Kishigami A, Sokabe M, Kojima I, Sato S, et al (2007) Arabidopsis plasma membrane protein crucial for Ca^{2+} influx and touch sensing in roots. Proc Natl Acad Sci USA **104:** 3639–3644

Ogasawara Y, Kaya H, Hiraoka G, Yumoto F, Kimura S, Kadota Y, Hishinuma H, Senzaki E, Yamagoe S, Nagata K, et al (2008) Synergistic activation of the Arabidopsis NADPH oxidase AtrbohD by Ca^{2+} and phosphorylation. J Biol Chem **283:** 8885–8892

Oparka KJ, Wright KM (1988a) Osmotic regulation of starch synthesis in potato tubers. Planta **174:** 123–126

Oparka KJ, Wright KM (1988b) Influence of cell turgor on sucrose partitioning in potato tuber storage tissues. Planta **175:** 520–526

Osuna D, Usadel B, Morcuende R, Gibon Y, Bläsing OE, Höhne M, Günter M, Kamlage B, Trethewey R, Scheible WR, et al (2007) Temporal responses of transcripts, enzyme activities and metabolites after adding sucrose to carbon-deprived Arabidopsis seedlings. Plant J **49:** 463–491

Paredez AR, Somerville CR, Ehrhardt DW (2006) Visualization of cellulose synthase demonstrates functional association with microtubules. Science **312:** 1491–1495

Passonneau JV, Lowry OH (1993) Enzymatic Analysis: A Practical Guide. Biological Methods. Humana Press, Totowa, NJ

Paul MJ, Foyer CH (2001) Sink regulation of photosynthesis. J Exp Bot **52:** 1383–1400

Peng L, Hocart CH, Redmond JW, Williamson RE (2000) Fractionation of carbohydrates in Arabidopsis root cell walls shows that three radial swelling loci are specifically involved in cellulose production. Planta **211:** 406–414

Pfaffl MW, Horgan GW, Dempfle L (2002) Relative Expression Software Tool (REST) for group-wise comparison and statistical analysis of relative expression results in real-time PCR. Nucleic Acids Res **30:** e36

Rajangam AS, Kumar M, Aspeborg H, Guerriero G, Arvestad L, Pansri P, Brown CJ, Hober S, Blomqvist K, Divne C, et al (2008) MAP20, a microtubule-associated protein in the secondary cell walls of hybrid aspen, is a target of the cellulose synthesis inhibitor 2,6-dichlorobenzonitrile. Plant Physiol **148:** 1283–1294

Reinhold T, Alawady A, Grimm B, Beran KC, Jahns P, Conrath U, Bauer J, Reiser J, Melzer M, Jeblick W, et al (2007) Limitation of nocturnal import of ATP into Arabidopsis chloroplasts leads to photooxidative damage. Plant J **50:** 293–304

Reiser V, Raitt DC, Saito H (2003) Yeast osmosensor Sln1 and plant cytokinin receptor Cre1 respond to changes in turgor pressure. J Cell Biol **161:** 1035–1040

Rogers LA, Dubos C, Cullis IF, Surman C, Poole M, Willment J, Mansfield SD, Campbell MM (2005) Light, the circadian clock, and sugar perception in the control of lignin biosynthesis. J Exp Bot **56:** 1651–1663

Rook F, Corke F, Card R, Munz G, Smith C, Bevan MW (2001) Impaired sucrose-induction mutants reveal the modulation of sugar-induced starch biosynthetic gene expression by abscisic acid signalling. Plant J **26:** 421–433

Sanevas N, Sunohara Y, Matsumoto H (2007) Characterization of reactive oxygen species-involved oxidative damage in Hapalosiphon species crude extract-treated wheat and onion roots. Weed Biol Manage **7:** 172–177

Scheible WR, Eshed R, Richmond T, Delmer D, Somerville C (2001) Modifications of cellulose synthase confer resistance to isoxaben and thiazolidinone herbicides in Arabidopsis Ixr1 mutants. Proc Natl Acad Sci USA **98:** 10079–10084

Seifert GJ, Blaukopf C (2010) Irritable walls: the plant extracellular matrix and signaling. Plant Physiol **153:** 467–478

Smith SM, Fulton DC, Chia T, Thorneycroft D, Chapple A, Dunstan H, Hylton C, Zeeman SC, Smith AM (2004) Diurnal changes in the transcriptome encoding enzymes of starch metabolism provide evidence for both transcriptional and posttranscriptional regulation of starch metabolism in Arabidopsis leaves. Plant Physiol **136:** 2687–2699

Stitt M, Lunn J, Usadel B (2010) Arabidopsis and primary photosynthetic metabolism: more than the icing on the cake. Plant J **61:** 1067–1091

Sulpice R, Pyl ET, Ishihara H, Trenkamp S, Steinfath M, Witucka-Wall H, Gibon Y, Usadel B, Poree F, Piques MC, et al (2009) Starch as a major integrator in the regulation of plant growth. Proc Natl Acad Sci USA **106:** 10348–10353

Sulpice R, Tschoep H, von Korff M, Büssis D, Usadel B, Höhne M, Witucka-Wall H, Altmann T, Stitt M, Gibon Y (2007) Description and applications of a rapid and sensitive non-radioactive microplate-based assay for maximum and initial activity of D-ribulose-1,5-bisphosphate carboxylase/oxygenase. Plant Cell Environ **30:** 1163–1175

Torres MA, Dangl JL, Jones JD (2002) Arabidopsis gp91phox homologues AtrbohD and AtrbohF are required for accumulation of reactive oxygen intermediates in the plant defense response. Proc Natl Acad Sci USA **99:** 517–522

Tran LS, Urao T, Qin F, Maruyama K, Kakimoto T, Shinozaki K, Yamaguchi-Shinozaki K (2007) Functional analysis of AHK1/ATHK1 and cytokinin receptor histidine kinases in response to abscisic acid, drought, and salt stress in Arabidopsis. Proc Natl Acad Sci USA **104:** 20623–20628

Tsang DL, Edmond C, Harrington JL, Nühse TS (2011) Cell wall integrity controls root elongation via a general 1-aminocyclopropane-1-carboxylic acid-dependent, ethylene-independent pathway. Plant Physiol **156:** 596–604

Valerio C, Costa A, Marri L, Issakidis-Bourguet E, Pupillo P, Trost P, Sparla F (2011) Thioredoxin-regulated beta-amylase (BAM1) triggers diurnal starch degradation in guard cells, and in mesophyll cells under osmotic stress. J Exp Bot **62:** 545–555

Wormit A, Trentmann O, Feifer I, Lohr C, Tjaden J, Meyer S, Schmidt U, Martinoia E, Neuhaus HE (2006) Molecular identification and physiological characterization of a novel monosaccharide transporter from *Arabidopsis* involved in vacuolar sugar transport. Plant Cell **18:** 3476–3490

Xie YJ, Xu S, Han B, Wu MZ, Yuan XX, Han Y, Gu QA, Xu DK, Yang Q, Shen WB (2011) Evidence of Arabidopsis salt acclimation induced by up-regulation of HY1 and the regulatory role of RbohD-derived reactive oxygen species synthesis. Plant J **66:** 280–292

Yandeau-Nelson MD, Laurens L, Shi Z, Xia H, Smith AM, Guiltinan MJ (2011) Starch-branching enzyme IIa is required for proper diurnal cycling of starch in leaves of maize. Plant Physiol **156:** 479–490

Yoshimura K, Miyao K, Gaber A, Takeda T, Kanaboshi H, Miyasaka H, Shigeoka S (2004) Enhancement of stress tolerance in transgenic tobacco plants overexpressing Chlamydomonas glutathione peroxidase in chloroplasts or cytosol. Plant J **37:** 21–33

Zhu J, Lee BH, Dellinger M, Cui X, Zhang C, Wu S, Nothnagel EA, Zhu JK (2010) A cellulose synthase-like protein is required for osmotic stress tolerance in Arabidopsis. Plant J **63:** 128–140

Zhu JK, Shi J, Singh U, Wyatt SE, Bressan RA, Hasegawa PM, Carpita NC (1993) Enrichment of vitronectin-like and fibronectin-like proteins in NaCl-adapted plant cells and evidence for their involvement in plasma-membrane cell-wall adhesion. Plant J **3:** 637–646